Stimulus-Induced Changes of Reflectivity Detected by Optical Coherence Tomography in Macaque Retina

Wataru Suzuki,[1–3] Kazushige Tsunoda,[1,2] Gen Hanazono,[1,2] and Manabu Tanifuji[2]

[1]Laboratory of Visual Physiology, National Institute of Sensory Organs, Tokyo, Japan
[2]Laboratory for Integrative Neural Systems, RIKEN Brain Science Institute, Saitama, Japan
[3]Department of Ultrastructural Research, National Institute of Neuroscience, National Center of Neurology and Psychiatry, Tokyo, Japan

Correspondence: Kazushige Tsunoda, Laboratory of Visual Physiology, National Institute of Sensory Organs, 2-5-1, Higashigaoka, Meguro-ku, Tokyo, 152-8902, Japan; tsunodakazushige@kankakuki.go.jp.

Submitted: May 10, 2013
Accepted: August 15, 2013

Citation: Suzuki W, Tsunoda K, Hanazono G, Tanifuji M. Stimulus-induced changes of reflectivity detected by optical coherence tomography in macaque retina. *Invest Ophthalmol Vis Sci*. 2013;54:6345–6354. DOI: 10.1167/iovs.13-12381

Purpose. To investigate the properties and origin of retinal intrinsic signals by functional optical coherence tomography (fOCT) in macaque retinas.

Methods. We modified a spectral domain OCT system to be able to give short-duration flashes or continuous light stimulation to the retina of three adult macaque monkeys (*Macaca mulatta*) under general anesthesia. Changes in the intensities of the OCT signals following the stimulus were determined.

Results. Stimulus-evoked decreases or increases in the OCT signals were observed in the photoreceptor inner segment ellipsoids and outer segments, respectively. Experiments with focal and colored stimuli confirmed that these fOCT signals originated from the photoreceptors. No diffuse changes in the OCT signals were detected in the inner retinal layers; however, there were slow changes in small discrete areas where the retinal vessels were located. The polarity of the fOCT signals in the inner retinal layer was dependent on each activated region, and one of the possible sources of the reflectance changes was the light-scattering changes of the retinal vessels.

Conclusions. The fOCT signals in the macaque retina consist of at least three components: light-scattering changes from the photoreceptor inner segment ellipsoids, light-scattering changes from the outer segments, and slow light-scattering changes from the blood vessels in the inner retina. This technique has the potential of mapping local neuronal activity three-dimensionally and may help in the diagnosis of retinal disorders of different retinal origins.

Keywords: OCT, retina, intrinsic signal, functional OCT, macaque

Although recent advances in imaging techniques, for example, scanning laser ophthalmoscopy (SLO), optical coherence tomography (OCT),[1–3] and fundus autofluorescence (FAF),[4] have revealed the morphology of retinal structures with fine spatial resolution, direct assessments of neuronal activities in the retina are possible only by electrophysiological techniques such as electroretinography and electrooculography. Recently, intrinsic signal imaging techniques have been used to create topographical maps of the cone- and rod-generated responses in macaque monkeys,[5–9] in humans,[10–12] in frogs,[13–16] and in cats.[17,18]

In a series of experiments on the intrinsic signals of the macaque's retina, we found that several types of signals with different origins could be evoked in the posterior retina by a bright flash stimulus: fast retinal signals at the fovea, fast and slow retinal signals away from the fovea, and slow signals at the optic disc.[5–9] The complex properties of the retinal intrinsic signals indicated that the flash-evoked intrinsic signals arose from a combination of light reflectance changes occurring independently and concurrently in the photoreceptor layer to the retinal ganglion cell (RGC) layer. However, the specific retinal layer from which the signals originated has not been determined because the instruments used to obtain the intrinsic signals did not have sufficient depth resolution.

Optical coherence tomography can provide high-resolution images of the high-light-scattering tissues at different depths in situ, and it has been used to evaluate local neuronal activities by measuring the stimulus-dependent light-scattering changes in the cerebral cortex.[19–21] This technique is referred to as functional OCT (fOCT), and several attempts have been made to map the neuronal activities of the retina by this technique.[22–30] Functional OCT is more advantageous than conventional intrinsic signal imaging because there are retinal disorders that primarily affect specific layers of the retina: rod–cone and cone–rod dystrophies for the photoreceptor layer, complete or incomplete congenital stationary night blindness for the middle layer of the retina, and glaucoma for the inner retina. However, in early studies, the characteristics of the fOCT signals including the signal polarities were different for different animals.[22–30] Before this technique can be brought into clinical use, more detailed physiological characteristics need to be confirmed in retinas that have the same properties as human retinas.

Thus, the purpose of this study was to determine the characteristics of the retinal intrinsic signals in the different retinal layers. To accomplish this, we developed an fOCT system and measured the stimulus-evoked signals that originated from distinct layers of the macaque retina in vivo. With this model, we have confirmed that the fOCT signals consisted of

fast light-scattering changes of the photoreceptor inner segment ellipsoids (ISe) and outer segments (OS), and the cone- and rod-induced responses could be separated. We also found that light stimulation induced slow light-scattering changes in scattered punctate regions of the inner retina. We suggest that these signals arose from reflectance changes of the blood vessels during and following neuronal activities.

Materials and Methods

Animal Preparation

The experiments were performed on three rhesus monkeys (*Macaca mulatta*). After an intramuscular injection of atropine sulfate (0.08 mg/kg), the monkeys were anesthetized with droperidol (0.25 mg/kg) and ketamine (5.0 mg/kg) and then paralyzed with vecuronium bromide (0.1–0.2 mg/kg/h). To reduce pain, fentanyl citrate (0.40 μg/kg/h) was continuously infused through the lesser saphenous vein. The monkeys were artificially ventilated with a mixture of 70% N_2O, 30% O_2, and 1.0% to 1.5% of isoflurane. The electroencephalograms (EEGs), electrocardiograms (ECGs), expired CO_2, and rectal temperature were monitored continuously throughout the experiments. The end-tidal CO_2 was set between 4.0% and 4.4% during the entire experiment. The O_2 saturation level was monitored by a pulse oximeter (Ohmeda 4700 Oxicap; Soma Technology Inc., Bloomfield, CT) at the fingertip and was approximately 95% during the recording and interrecording periods. Before the recordings, the pupils were fully dilated with topical tropicamide (0.5%) and phenylephrine hydrochloride (0.5%). Each experiment lasted 7 to 8 hours, including the time for the preparation of the animals.

The experimental protocol was approved by the Experimental Animal Committee of the RIKEN Institute, and all experimental procedures were carried out in accordance with the guidelines of the RIKEN Institute and the ARVO Statement for the Use of Animals in Ophthalmic and Vision Research.

Functional OCT System

The original spectral domain OCT system was built to include a digital fundus camera system (NM-1000; Nidek, Aichi, Japan). The optical pathway was split in two; one-half of the light passed to the OCT system and one-half to a flood illumination fundus camera system. The spectrometer of the OCT system was adapted for a broadband superluminescent diode (SLD) light source (central wavelength 890 nm, bandwidth 50 nm; Superlum Diodes, Ltd., Co Cork, Ireland), resulting in an approximate 5-μm axial resolution in tissue. The optical power of the beam at the cornea was 700 μW, which is lower than the American National Standards Institute exposure limit. The size of the beam on the cornea was 1.8 mm, resulting in an approximate 10-μm lateral resolution. B-scan images consisting of 1000 A-lines were taken along the horizontal or vertical meridians through the fovea or the optic disc. The length of the scan at the retina was approximately 9 mm with 1-μm overlap of neighboring A-lines. The scanning frequency of the galvanometer was 30 Hz. The spectrometer consisted of commercial compound lenses, a volume phase holographic transmission grating (1200 lpmm; Wasatch Photonics, Inc., Logan, UT), and a high-speed line charge-coupled device (CCD) camera (AViiVA SM2 CL 101x; Atmel, San Jose, CA). The line CCD camera was configured with a line rate of 53,000 A-lines per second, with 1024 pixels and 12-bit gray-level resolution. The sensitivity of this system was approximately 93 dB with 700 μW of incident power on the cornea.

The stimulation system was embedded in the optical pathway of the flood illumination fundus camera system.[5,6] The retina was stimulated with either an unfiltered xenon flash of 1-ms duration, or a continuous (steady) illumination from a halogen lamp filtered through a monochromatic green filter ($\lambda_{max} = 500 \pm 15$ nm) for stimulation of mainly the rods, or a yellow filter ($\lambda_{max} = 590 \pm 15$ nm) for the stimulation of mainly the M/L-cones.[31,32]

Experimental Protocol

Each trial consisted of 300 or 480 B-scan images collected at 30 frames per second for a total recording time of 10.0 or 16.0 seconds. To reduce the respiration-induced periodic movements of the eye, the respirator was stopped during the recording period. In the experiments with a xenon flash (Figs. 1, 2), a flash stimulus was given 1.0 or 2.0 seconds after the initiation of data acquisition. The maximum flash intensity (0 log units) measured at the cornea was 308.0 cd·s/m^2 (measured at 50.2 mm from the objective lens, by model IL-1700 photoradiometer; International Light Technologies, Inc., Peabody, MA). The timing of the data acquisition and stimulus delivery was under computer control. The interval between trials was 30 minutes for flash stimuli and 60 minutes for continuous stimuli. During the intertrial periods, the retina was kept under dark-adapted conditions.

A focal stimulus was projected onto the retina by inserting a transparent film in the optical pathway of the xenon strobe[6] (Fig. 2A). The film was placed at a point that was conjugate to the retina. The shape and size of the stimulus on the retina were determined by the pattern on the film. In the experiments with continuous stimulation (Figs. 3, 4), the retina was stimulated with light that passed through either the green or yellow filter 0.5 seconds prior to data acquisition. The light intensity was unchanged throughout the recording period (green, 6.54 log scot. td; yellow, 5.35 log phot. td). The OCT signals were recorded for 16.0 seconds. The interval between trials was 60 minutes.

Data Analyses

We evaluated the changes of the OCT signals that were evoked by the light stimuli for each pixel by comparing the OCT images with those recorded at the beginning of each trial. The differential OCT signals, $\Delta(x, z, t)$, were obtained by:

$$\Delta(x,z,t) = \frac{R(x,z,t) - \langle R(x,z)\rangle_{\text{pre}}}{\langle R(x,z)\rangle_{\text{pre}}}$$

where $R(x, z, t)$ is the reflectivity at position x and z at time t. $<R(x, z)>_{\text{pre}}$ is the average reflectivity during the prestimulus period of 1 or 2 seconds at position x and z for the trials with flash stimuli, or during the initial 0.5 seconds following data acquisition for the trials with continuous stimulation. For analysis of the OCT signals, values on a linear scale were always used.

The changes in the reflectance in each layer were evaluated by averaging the pixel values of 60 A-lines based on the segmentation of the retinal surface and ISe line. Before the segmentation, all OCT images in a trial were averaged (300 or 480 frames) and filtered by an averaging filter (4×4). For the averaged image, the border of the internal limiting membrane (ILM) was segmented by detecting the sudden change of signal intensity. The intensity peak of the ISe line was segmented by detecting the 0 crossing of the first derivative of the signal intensity (Fig. 1). To obtain the time course of the OCT signals, the results of two to five consecutive trials were averaged. The graphs of the time courses of the fOCT signals in Figures 1C,

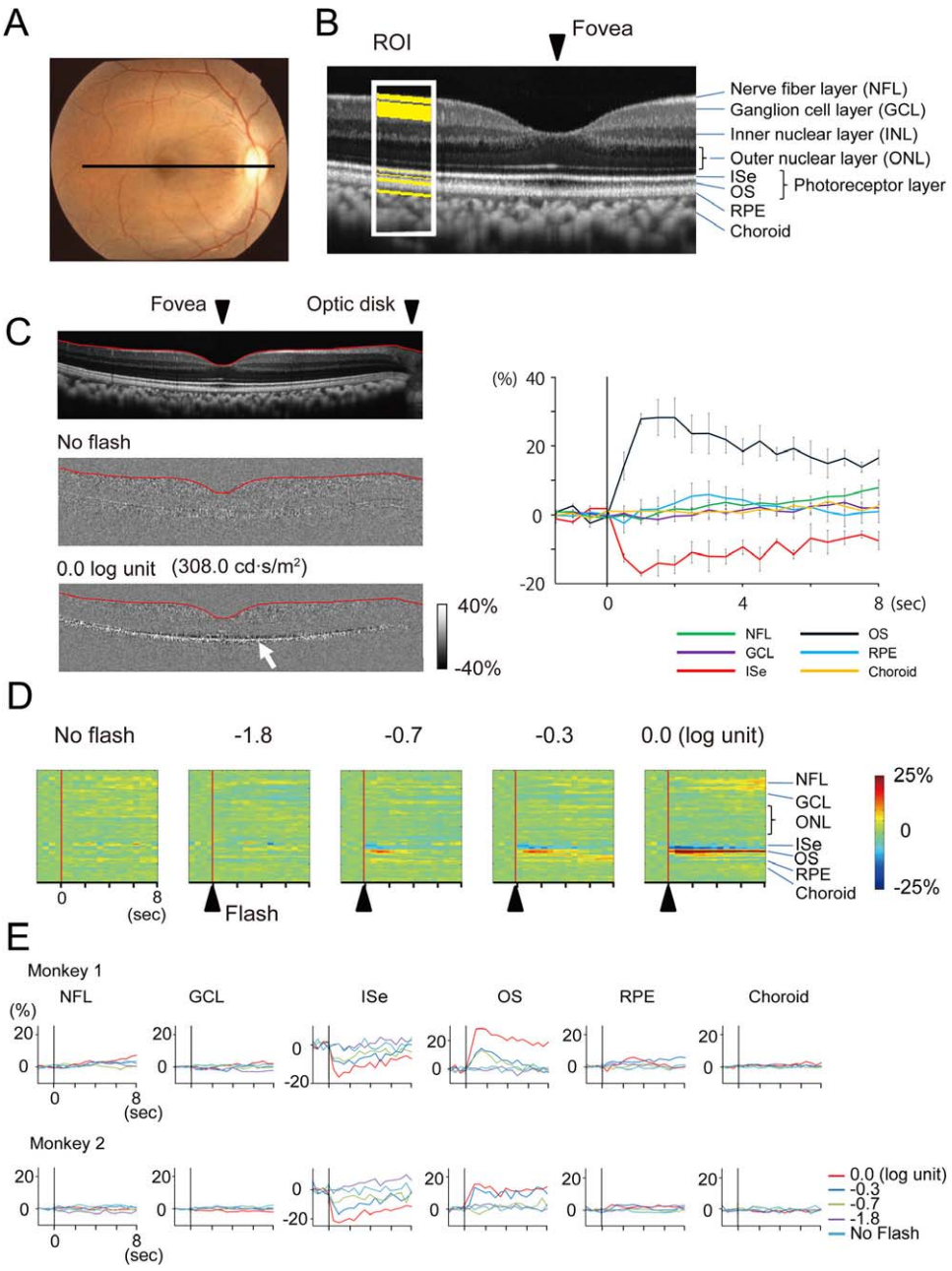

Figure 1. Flash-evoked intensity changes of the retina of monkeys 1 and 2. (**A**) The location of the horizontal scan line is indicated on the fundus image. (**B**) Horizontal profile of the central retina observed by OCT with the locations of the corresponding anatomical structures indicated. The location of the fovea is indicated by the *arrowhead*, and the region used for the time-course analysis in (**C**–**E**) is indicated by *yellow lines* in *white rectangle*. ISe, ellipsoid of photoreceptor inner segment; OS, photoreceptor outer segment. (**C**) *Top left*: Horizontal profile of the posterior retina observed by OCT. *Middle and bottom*: Differential images of fOCT showing the flash-evoked intensity changes (average of three trials). The fOCT images 1.0 seconds following white flash were divided, pixel by pixel, by those before the stimulus. The results without the flash (*middle left*) or with the white flash (*bottom left*) are shown in grayscale image. There are bands of decreased (*black*) or increased (*white*) reflectances in the photoreceptor layer (*arrow* in *bottom figure*). The locations of the fovea and optic disc are indicated by the *arrowheads*. The inner surface of the retina is marked by *red*. *Right*: Time courses of flash-evoked fOCT signals in different layers of the retina elicited by maximal flash intensity (0.0 log units) measured in the ROI in (**B**); nerve fiber layer (NFL), ganglion cell layer (GCL), ISe, OS, retinal pigment epithelium (RPE), and choroid. (**D**) Depth-resolved fOCT responses over time, horizontally averaged in a parafoveal region in (**B**). Responses without stimulation and with four different intensities of flash stimuli are shown. The flash was given at 0 seconds, which is indicated by the *arrowheads* and *vertical red lines*. The corresponding retinal layers are indicated on the *right*. With high-intensity (0.0 and −0.3 log unit) stimulations, there was an abrupt increase of the OCT signal in the photoreceptor outer segment (OS) and an abrupt decrease in the ellipsoid of photoreceptor inner segment (ISe) following the flash. There were also slow and weak increases of the OCT signals in the nerve fiber layer (NFL; 0.0 log units). (**E**) Time courses of flash-evoked fOCT signals in different layers of the retina measured in two monkeys; NFL, GCL, ISe, OS, RPE, and choroid. Responses elicited by different flash intensities (0.0 and −1.8 log units) are shown.

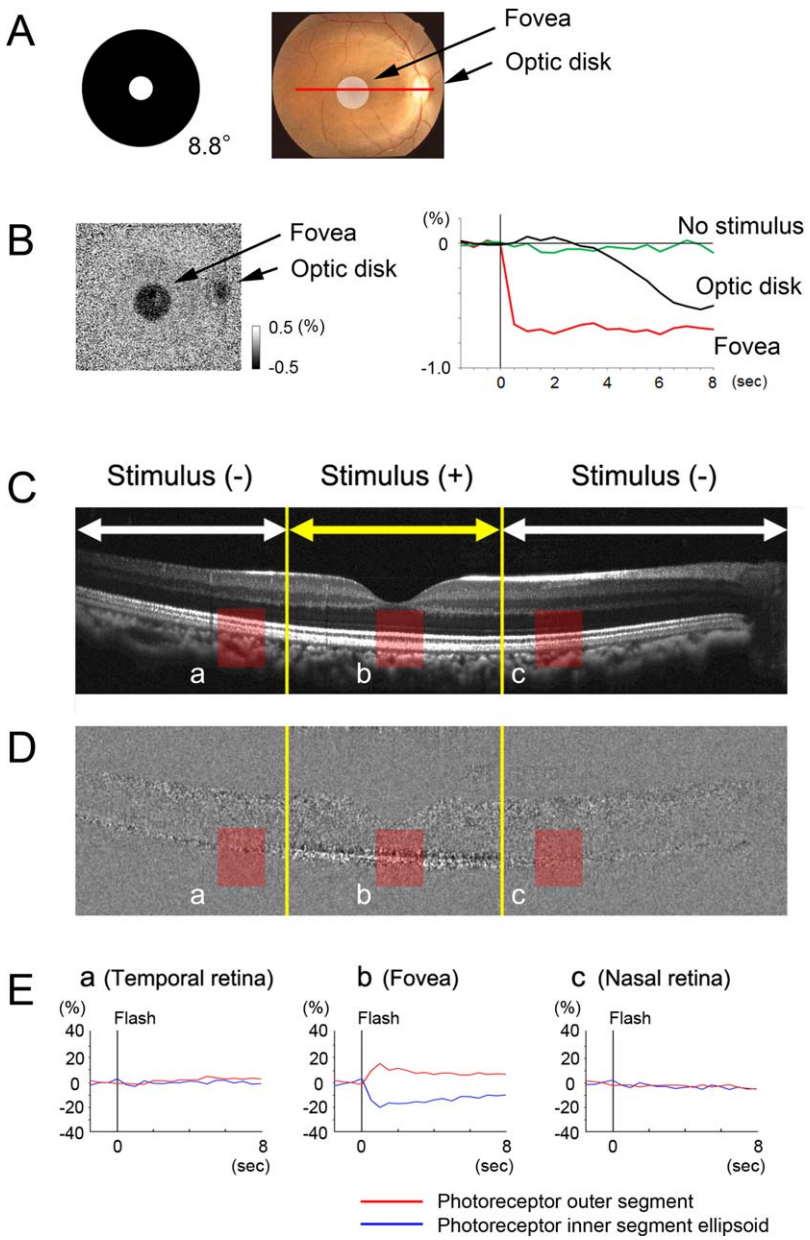

Figure 2. Intrinsic signals using fundus camera and fOCT signals induced by the same focal flash stimuli in monkey 3. (**A**) Circular focal stimulus (*left*) in the macular area including the fovea (8.8° in diameter) is shown on a fundus image at the *right*. (**B**) *Left*: Fundus image of intrinsic signal evoked by the focal stimulus, averaged from 0.5 to 3.0 seconds following stimulation. *Right*: Plot of the time courses of light reflectance changes following a focal flash at the fovea and the optic disc, and in a trial without flash at the fovea. Data from four consecutive trials were averaged. (**C**) Horizontal profile of the OCT image traversing both stimulated and nonstimulated regions of the retina. Regions for time-course analysis are indicated as (**a**) temporal retina, (**b**) fovea, and (**c**) nasal retina. (**D**) Differential images of the fOCT showing the flash-evoked intensity changes (average of three trials). The fOCT images during the initial 2 seconds following the white flash were divided, pixel by pixel, by those before the stimulus, and the results are shown in a grayscale image. There are bands of decreased (*black*) or increased (*white*) reflectance in the photoreceptor layer only at the stimulated region. (**E**) Plot of the time courses of light reflectance changes following a focal flash at the three locations shown in (**C**, **D**). Data from three consecutive trials were averaged.

1E, 2E, 3B, and 3D show the ratio of the reflectance changes to the baseline (%). A positive change indicates that the OCT signal increased following the stimulus, and a negative change indicates a decrease. Both positive and negative changes in the OCT signal were correlated with the neuronal responses. In the grayscale images shown in Figures 1C and 2D, the increase of OCT signal is represented by white and the decrease by black.

Because the OCT system we used has an approximate 5-μm axial resolution with a high dynamic range, eye movements can cause significant artifacts even though they are small. To compensate for the small variations in the cross-sectional position due to eye movements, we used correlation analysis. We selected the first frame of each trial as a reference, and calculated the coefficients of correlation between the reference signals of the first and following frames by changing the spatial position pixel by pixel. The frames were realigned to the spatial position that gave the highest correlation coefficient. The B-scan images were noted to shift periodically back and forth along the *z*-axis during each recording trial. This

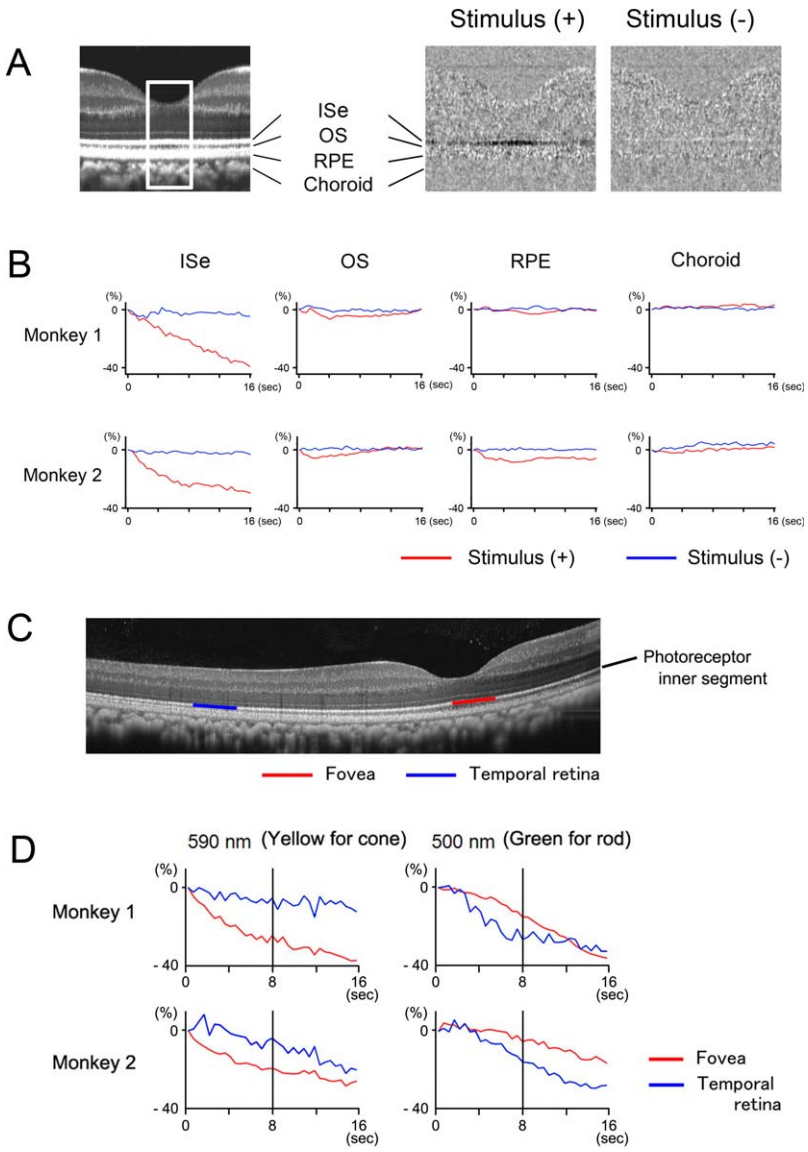

Figure 3. Time courses of fOCT signals induced by continuous/steady stimulation with different wavelengths of light in monkeys 1 and 2. (**A**) Foveal profile of fOCT image evoked by white continuous stimulus. The differential image is the average of 16 seconds of a single trial. (**B**) Time courses of fOCT signals evoked by white continuous stimulus from different retinal layers; photoreceptor inner segment ellipsoid (ISe), photoreceptor outer segment (OS), retinal pigment epithelium (RPE), and choroid. (**C**) Foveal and temporal retinal regions for the photoreceptor inner segments for the time-course analysis. The center of the stimulus was focused between the two recorded regions so that light intensity and incident angle of the stimulus were equal at the two regions. *Red*: fovea; *blue*: temporal retina. (**D**) Time courses of fOCT signals in the ISe following continuous stimulation by yellow (590 nm) or blue-green (500 nm) illumination measured in the two retinal locations in (**C**). With yellow illumination, fOCT signals are more rapidly evoked at the fovea than at the temporal retina. With green illumination, fOCT signals are more rapidly evoked at the temporal retina than at the fovea.

movement completely matched the heartbeats, so its origin was considered to be the pulsation of intra- and extraocular arteries. The magnitude of this back-and-forth movement was only 1 to 2 pixels along the *z*-axis (Supplementary Fig. S1), and the estimated difference of the OCT intensities due to one pixel shift (5 μm in the retinal depth) was at most 0.3%. Thus, we believe that fOCT changes of ~20% were not significantly influenced by eye movements during a recording trial.

To confirm the locations of small blood vessels, we measured the blood flow using a phase-sensitive method (Fig. 5).[33] We used the same imaging device as for the fOCT, but the lateral width for imaging was reduced by one-half. The overlap of two neighboring A-scans was twice that for the fOCT imaging. The signals detected by the line CCD camera (AViiVA SM2 CL 101x; Atmel) were interpolated to generate a spectrum with points linear in k-space. Information on the depth-resolved intensity and phase was obtained by Fourier transforming the spectrum for each A-line. Doppler OCT images were obtained by calculating the phase difference between points at the same depth in adjacent A-lines.

The correspondence between the hyperreflective band in the photoreceptor layer and the anatomy is still under debate, for example, the junction between the IS and OS[34] or the IS ellipsoid.[35,36] We are aware of this debate, and to avoid confusion we have used the term IS ellipsoid (ISe) for this hyperreflective band below the external limiting membrane (ELM).

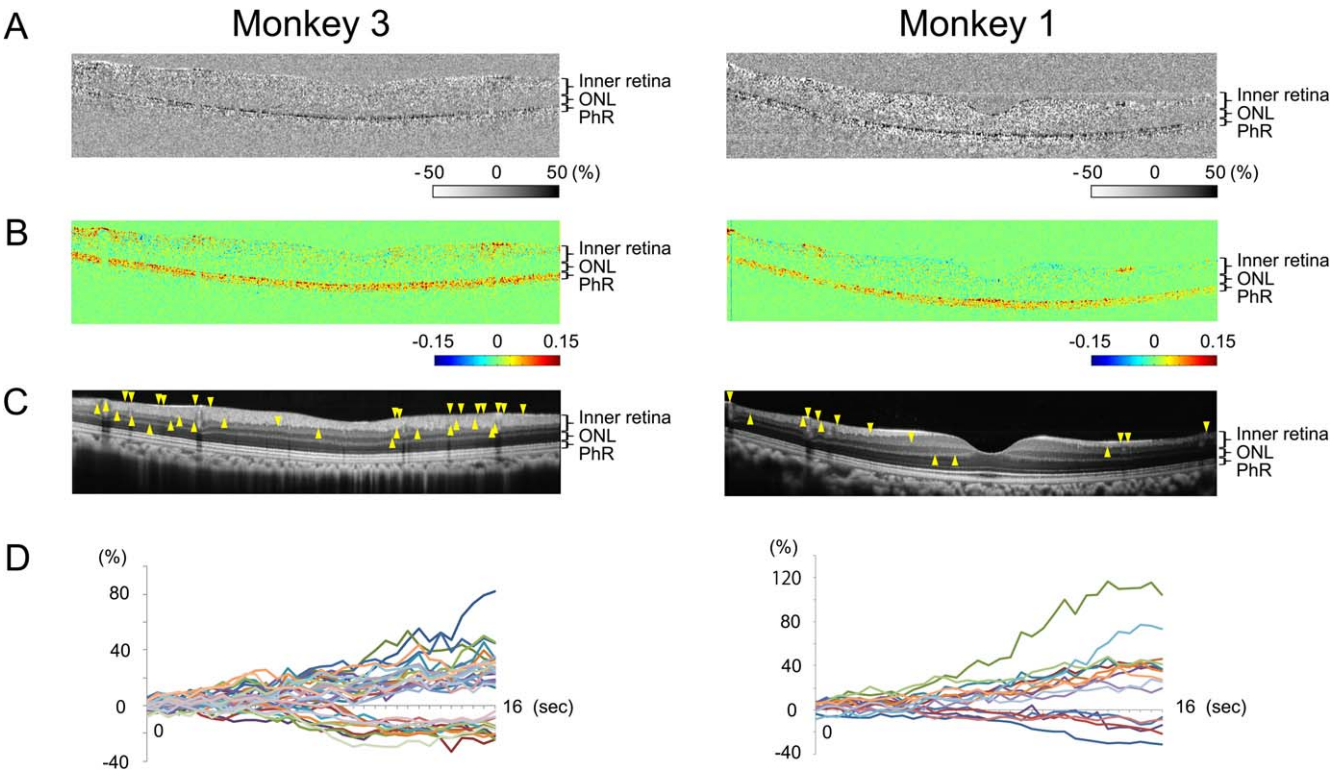

Figure 4. Distribution of discrete regions that had an increase or a decrease of the OCT intensity following steady stimulation (monkeys 3 and 1). (**A**) Differential OCT images shown in grayscale (average of five trials). OCT images at 16 seconds after the stimulus were divided by those during the initial 500 ms following data acquisition. Decreased OCT signal is shown by *black*, and increased OCT signal is shown by *white*. (**B**) Pseudo-color maps showing the coefficients of variation (CV; standard deviation divided by mean) of the fOCT intensity of the individual pixels during 16 seconds following the stimulus relative to those without the stimulus. *Red pixels* indicate regions where poststimulus variance of the signal was large. There are wide horizontal bands of high variance in the photoreceptor layer (PhR) and small regions with high variance scattered in the inner retina. (**C**) Regions that showed larger variances in the OCT intensity of more than 3 SDs of the spatially averaged CV in the whole retina. Band-like regions with high variance in the photoreceptor layer (PhR) in (**B**) were excluded from this analysis. Thirty-four regions from monkey 3 and 15 regions from monkey 1 were found in the inner retina (*arrowheads*). Some of the regions matched the locations of retinal vessels. There were no regions with high variance in the outer nuclear layer (ONL). (**D**) Time courses of the fOCT signals in localized regions in (**C**). The OCT intensity either increased or decreased gradually following the stimulus.

Results

The differential fOCT images showing the flash-evoked intensity changes and the time course of the flash-evoked fOCT signals are presented in Figure 1. The time courses of the fOCT images in Figures 1D and 1E were obtained from the rectangular region (ROI) in Figure 1B.

Following the flash stimulus, changes in the fOCT signals were observed in both the ISe and OS layers of the photoreceptors. However, the polarities of these signals were reversed (Figs. 1C, 1D, 1E). The OCT intensities in the ISe layer decreased by approximately 20.0%, while the OCT intensities in the OS increased by approximately 15.0% to 30.0% following the highest stimulus intensity (Figs. 1C, 1E). The time of the peak intensity change for both of these signals was approximately 1.0 seconds, and the signal gradually returned to the baseline. The absolute value of the signal intensity in the photoreceptor layer was proportional to the flash stimulus intensities.

In the other layers, for example, nerve fiber layer (NFL), ganglion cell layer (GCL), outer nuclear layer (ONL), retinal pigment epithelium (RPE), and choroid, fast stimulus-induced changes of the fOCT signals were not observed as in the photoreceptor layer (Figs. 1C, 1D, 1E).

Earlier, we showed that focal flash stimuli evoked fast light-scattering changes only in the stimulated region.[6] This was also confirmed in the fOCT images. We stimulated focal regions of the posterior retina, and measured 1) the intrinsic signals using the infrared fundus camera (Fig. 2B)[5,6] and 2) the fOCT signals (Figs. 2C, 2D, 2E) from the same retinal location. We compared the time courses of the flash-evoked signals in both the stimulated and nonstimulated regions under dark-adapted conditions. The macular area including the fovea was focally stimulated with an 8.8° circular stimulus (Fig. 2A). In the fundus camera–based intrinsic signal imaging, the intrinsic signal was observed in the stimulated region as a light reflectance decrease at both the fovea and optic disc (Fig. 2B). In the fOCT images, the intrinsic signal was observed in the stimulated region as either a decrease in the ISe layer or an increase in the OS layer (Figs. 2D, 2E). The time course of intrinsic signals in the stimulated region in the image obtained by the fundus camera almost matched that of the ISe and OS in the fOCT images, although the polarity was opposite in the OS. The temporal and nasal regions that were not stimulated did not show changes in their reflectivity following the stimulus.

To further confirm that photoreceptor activity contributed to the fOCT signals, the ISs were determined for different retinal locations and different wavelengths of the stimulus (Fig. 3). The λ_{max} of the spectral sensitivity of the middle- and long-wavelength cones is at approximately at 535 nm and 565 nm, respectively, and the λ_{max} of the rod photoreceptors is at approximately 500 nm.[31,32,37] Thus, we used yellow light with a peak wavelength transmission at 590 nm and blue-green light with a peak wavelength transmission at 500 nm. For this study,

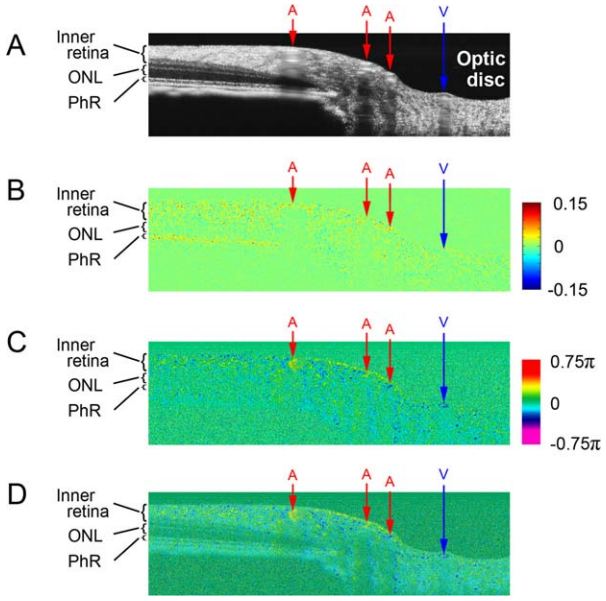

Figure 5. Doppler OCT imaging showing the location of retinal vessels in monkey 3. (**A**) Horizontal profile of structural OCT image temporal to the optic disc. Retinal arteriole (A) and venule (V) are marked by *arrows*. (**B**) Flash-evoked fOCT images at the same location as in (**A**). Pseudo-color maps show the coefficients of variation (CV; standard deviation divided by mean) of the OCT intensity of the individual pixels as in Figure 4B. *Red pixels* indicate regions where poststimulus variance of the signal was large. There are horizontal bands of high variance in the photoreceptor layer (PhR) and small regions with high variance scattered in the inner retina. (**C**) Doppler OCT image averaged over five B-scan images in the same location as in (**B**). The magnitude of the phase shift is indicated by a *pseudo-color scale*. (**D**) Overlaid image of structural image in (**A**) and Doppler OCT image in (**C**). The locations of bidirectional flow correspond to those of retinal arterioles and venules (*arrows*). Retinal capillaries were observed as punctate small regions with blood flow in the inner retina.

we used continuous and steady stimuli instead of short-duration flash stimuli because the intensity of the colored flash stimuli through narrow bandpass filters was not intense enough to evoke stable responses at the photoreceptor layer. With white continuous stimuli, a gradual decrease in OCT reflectance was observed in the ISe layer (Figs. 3A, 3B). The reflectance change was as large as 30% at the end of the trial. In the OS, however, an increase in the OCT reflectance was not observed as in the trials with flash stimuli. We thus evaluated the photoreceptor responses from the ISe for colored stimulation.

With the yellow stimulus, the response of the photoreceptor ISes during the initial recording period was greater at the fovea than at the temporal retina; with the blue-green stimulus, the response was greater at the temporal retina than at the fovea (see the vertical lines at 8-second intervals following the stimulus). Cones are most densely packed at the fovea, while the density of the rods is highest in the perimacular region.[37–39] Although the data appear less quantitative because the averaging between the different trials was difficult with this recording protocol, our results indicate the difference in anatomical distribution of both cone and rod photoreceptors. These results support the idea that the fOCT signals arose from activity-dependent reflectance changes in the ISes and not from optical artifacts.[31,32,37]

In the differential image following spatial averaging, fast fOCT responses after stimulation were not observed in the inner retina (Fig. 1C, left). However, if a specific small area was selected for a time-course analysis, slow increases of the reflectance could be detected in the NFL and GCL (Figs. 1D, 1E, at 0.0 log units). To evaluate these slow fOCT signal changes in the inner retina, we calculated the coefficient of variation (CV, standard deviation/mean of the OCT signals) for each pixel during the recording period. We subtracted the CVs for the nonstimulated trials from those in stimulated trials, and these subtracted CV values are plotted in Figure 4B. Pixels with higher variances of the fOCT signals (>3 SDs of the mean of the subtracted CV values in the entire B-scan image) were examined for the entire recording area except the photoreceptor layer. We found 34 regions in monkey 3 (vertical profile between fovea and optic disc) and 15 regions in monkey 1 (vertical profile of the fovea) that were scattered in the inner retina (Fig. 4C). The time course of the changes in the reflectance in the regions with higher variance is plotted in Figure 4D following a spatial averaging of 5 × 5 pixels. The OCT signal in these regions either increased or decreased slowly following the stimulus. In this experiment, continuous and steady stimuli were used. However, slow time-course signals were equally observed when brief flash stimuli were used. Some of the regions with slow fOCT signals were confirmed to match the locations of superficial retinal vessels, but others did not match (Fig. 4C). With the spatial resolution of our instrument, we could not distinguish individual arterioles, venules, and capillaries that were located away from the ILM. However, it was notable that the distribution of scattered regions with high fOCT signal variances matched that of retinal vessels in the inner retina. There were no regions with high variance in the ONL, which is known to be a region without retinal vessels.[40] These results suggested that there were regions in the inner retina with retinal vessels that had slow OCT signal changes, which could be either increases or decreases in the reflectance. Because the individual active regions in the inner retina were small, we could not observe fOCT responses in the spatially averaged differential images (Fig. 1C, left).

To confirm the contribution of retinal vessels to the slow fOCT signals shown in Figure 4, we measured both the fOCT and blood flow by a phase-sensitive method.[33,41,42] The measurements were made from regions near the optic disc where the retinal arterioles and venules can be clearly seen (Fig. 5). The Doppler OCT images that were averaged over five B-scan images (167 ms) are shown in Figure 5C. This Doppler OCT image was overlaid by the structural OCT image in Figure 5D. The locations of bidirectional flow in the Doppler OCT image marked by A or V matched those of the retinal arterioles and venules in Figure 5A. Capillaries were observed as punctate regions with blood flow in the inner retina (Fig. 5D). The overall location of the retinal capillaries matched that of the punctate-active regions in the fOCT images (Fig. 5B). However, the correspondence between locations of independent capillaries and active fOCT regions could not be determined in the Doppler OCT images due to the reduced spatial resolution.

Discussion

The properties of the fOCT signals in the macaque retina, which has structural and physiological properties similar to those of the human retina, were determined. As best we know, this is the first investigation of these properties. The intensity-dependent fOCT signals were observed in the photoreceptor layer (Fig. 1), and the relationship between the photoreceptor activities and the reflectance changes was further confirmed by measuring focal responses (Fig. 2) and wavelength-dependent responses (Fig. 3) in the photoreceptor layer. In addition, we

Investigative Ophthalmology & Visual Science

showed that there were scattered punctate regions with very slow reflectance changes in the inner retina (Figs. 4, 5).

There have been fOCT studies of the retina of frogs,[22] rabbits,[23] rats,[24] and chickens.[29] It is interesting that the characteristics of the fOCT signals, including the signal polarities, were different among these animals. Yao et al.[22] measured the flash-evoked reflectivity changes of the OCT images from isolated frog retinas and observed an increase in reflectivity (positive fOCT signals) in the GCL and decreased reflectivity (negative fOCT signals) in the photoreceptor layer. Bizheva et al.[23] found negative fOCT signals in the ISes and positive signals in the OS following flash stimuli in isolated rabbit retinas. Srinivasan et al.[24] demonstrated positive fOCT signals in the OS following steady stimulation (1.3 seconds), but negative fOCT signals were not observed in the ISes of the in situ rat retina. Moayed et al.[29] examined chicken retinas in situ and compared fast fOCT signals within 50 ms following a flash with the ERG responses. They found a decrease of reflectivity in the OS and RPE (peak at 34 ms after the flash) and an increase of reflectivity in the NFL and GCL (peak at 33 ms after the flash). They concluded that these fOCT signals were strongly linked with the fast electrophysiological activity of the ERGs. They also observed slow negative fOCT signals after 100 ms as reported in other studies, including our study. They attributed these slow signals to photoreceptor regeneration, blurring of the image beam due to pupil contraction, and visually evoked constriction of the chicken retina. As mentioned earlier, the characteristics of the intrinsic signals measured by fOCT varied in the different studies. This may be due to differences not only in species but also in the recording instruments and protocols. In addition, the correspondence between OCT images and the anatomy has not been fully determined, and there is still a debate on the source of the hyperreflective band in the photoreceptor layer below the ELM. If this band is considered to be the junction between the IS and OS as suggested by Jonnal et al.,[34] the discrepancies in the results of fOCT in different publications would be less problematic. Thus, the origin of the fOCT signals should be carefully interpreted.

In our experiments, we estimated the photoreceptor OS responses from a low-reflectivity region between the two highly reflective lines in the photoreceptor layer, the ISe line and the cone outer segment tip (COST) line. This was done to exclude the potential contribution from the RPE because the COST line does not actually correspond to the "tip" of the photoreceptor OS but to the ensheathment of the cone OS by the apical processes of the RPE, that is, the contact cylinders.[36]

The fOCT signals of the macaque retina elicited by flash stimuli were similar to those reported by Bizheva et al.[23] in both the signal polarities and the time course—a negative signal in the ISes and a positive signal in OSs with peaks at 0.5 to 1.0 seconds. The origins of the fOCT responses in the photoreceptor layer had been thought to be related to the changes in optical properties following rapid membrane potential changes, or were secondary to microstructural changes such as cellular swelling and shrinking produced by ion fluxes following changes in the membrane polarization.[22,23,43,44] Recently, Moayed et al.[29] successfully detected fast fOCT signals from the in situ chicken retina, which were strongly linked to the rapid membrane potential changes. The fOCT signals we observed were much slower than the events directly linked to the ERG activities and may also reflect secondary changes following the early phototransduction processes, including the recovery of membrane potentials or photopigment regeneration. The difference in the polarity between the ISe and OS signals can be attributed to both structural and functional differences between the two structures. The ISes are composed of tightly packed mitochondria, which play important roles in metabolism during early visual processes, and OSs are composed of densely stacked discs that contain the photopigments essential for phototransduction. It is reasonable to think that the scattering properties following visual stimulation differ between these two layers, but the exact mechanism causing these changes cannot be determined from the results of our experiments with low temporal resolution.

What was notable in our experiments was that with a continuous steady stimulus, we observed only negative fOCT signals in the photoreceptor ISe, and the positive fOCT signals in the OS did not appear (Figs. 3A, 3B). We suggest that the fOCT signals in the OS may be more tightly coupled with brief and robust cellular reactions during the early visual processes than those in the ISe.

In conventional intrinsic signal imaging using a flood illumination camera, the negative intrinsic signals at the fovea would represent the combined reflectance changes from the ONL to the photoreceptor OS.[5,6,9] The time course of the ISe and OS signals in the stimulated region almost matched that with the conventional fundus camera, but the polarity in the OS was reversed (Fig. 2). The question then arises as to which layer of the retina is the major contributor to the conventional intrinsic signals, because the polarity of the functional signals in these two imaging techniques does not necessarily match. Yao and Zhao[13] and Yao et al.[22] measured the relatively slow intrinsic signals (peak; at ~1.0 seconds) by both fOCT and conventional near-infrared functional imaging using a flood illumination camera. The images were from the same retinal depth of isolate frog retinas.[13,15,22] These authors found that the polarity of the intrinsic signals in the photoreceptor layer was negative in both imaging systems. This implied that the negative reflectance changes in the ISe mainly contributed to the intrinsic signals obtained by the conventional flood illumination camera in macaques, although there is still a possibility of species differences.

Stimulus-evoked changes in the OCT reflectivity in the inner retina have been reported in isolated frog retinas[22] and in situ chicken retinas.[29] Moayed et al.[29] reported that fast fOCT signals of the inner retina that corresponded to the ERG responses were detected in chicken retinas with an increase of the OCT reflectivity (peak at 33 ms following a flash), followed by a decrease (peak at 69 ms) in both the NFL and GCL. The properties of the fOCT signals we found in the inner retina of macaque were much different from those reported by Yao et al.[22] and Moayed et al.[29] We found punctate regions with slow fOCT signals with either positive or negative polarity, and these were considered to be due to scattering of the measuring light in the inner retina. Some of the regions with slow fOCT signals were confirmed to match the locations of superficial retinal vessels by direct observations (Fig. 4C). Further analysis combined with Doppler OCT confirmed that the overall location of the punctate fOCT signals matched the location of retinal capillaries (Fig. 5). The discrete regions that showed the slow fOCT signals were found only in the inner retina where the retinal vessels are present.[40] This supported the idea that the origin of slow fOCT signals was from retinal vessels.

Arterioles in neural tissues, such as those in the retina and cerebral cortex, are rich in smooth muscle, and their contractions and relaxations are regulated by local neural activation through the glial cells; studies of isolated mammalian retinas and cortical tissues showed that light stimulation or glial cell stimulation can constrict or dilate arterioles.[45–49] We suggest that microstructural changes of the vessel walls during contraction or relaxation of smooth muscles were the most likely causes of the light-scattering changes in the tissue following light stimulation. Alternatively, a spatial shift of the vessels during vasodilation or vasoconstriction, or changes in

Investigative Ophthalmology & Visual Science

blood flow in the vessels, could also change the fOCT reflectivity. Stimulus-evoked activation of the retinal ganglion cells increases blood flow following vasodilation of the arterioles,[7,50] and the time course of the flow changes matches that of the slow fOCT signals.

The fOCT signals in each region of the inner retina had different polarities but similar time courses (Fig. 4D). The reason might be that the polarity of the reflectance changes depends on the incidence angle of the laser light on the vessel walls.[51] The retinal vessels run from the NFL to the outer plexiform layer in a very intricate pattern and form a complex three-dimensional network.[40,52] Thus, both the intensity and polarity of the slow reflectance changes probably differed depending on the location and direction of the vessels in the retina. In the rat somatosensory cortex, stimulus-dependent OCT signals also changed polarity[21]; however, the source of the signals has not been determined.

Fast fOCT signal changes were not detected in the RGC layer where stimulus-evoked spiking activities are present. This does not necessarily mean that changes in the fOCT signals did not occur in the RGCs. With greater improvement in the time and spatial resolutions, stimulus-evoked light-scattering changes not only from the vessels, but also from activated neurons and glial cells, could possibly be detected.[29] In any cases, it is difficult to draw any conclusions regarding the possible sources of fOCT signals in the inner retina with our recording technique.

The correspondence between the location of the independent capillaries and active fOCT regions could not be determined due to the limitation of spatial resolution. Our two-dimensional (2-D) cross-correlation algorithm is also limited with regard to reducing the noise due to eye movements because the retinal movements include not only motion in depth but also X–Y shift and rotation. Instead, 3-D rendering algorithms will surely enable better alignment and reduce motion-induced artifacts. However, our spectral domain OCT system with 53 kHz SLD takes 10 seconds to record one 3-D image of the ROI. This reduces the time resolution, which is very important for verifying the functional signals. More advanced techniques such as swept-source OCT and femtosecond laser OCT will be required to perform 3-D rendering algorithms for our experiments.

In summary, we have found that fOCT can detect layer-specific responses in the macaque retina following visual stimulation. The negative light-scattering changes of the fOCT in the photoreceptor ISe layer had response properties similar to those of faster intrinsic signals obtained by a conventional fundus camera. The properties of the fOCT signals in the inner retina partly matched slower intrinsic signals obtained by a conventional fundus camera, indicating that the responses are related to the vascular changes. At present, recording fOCT signals from human subjects is still challenging.[26–28] However, the information on the signal sources obtained in this study will make clinical application of this technique much more valuable and reliable for the diagnosis of various retinal disorders.

Acknowledgments

Supported in part by research grants from the SENTAN, Japan Science and Technology Agency (JST), Japan; research grants from the Ministry of Health, Labor and Welfare, Japan; and Grant-in-Aid for Scientific Research, Japan Society for the Promotion of Science, Japan. The authors alone are responsible for the content and writing of the paper.

Disclosure: **W. Suzuki**, None; **K. Tsunoda**, None; **G. Hanazono**, None; **M. Tanifuji**, None

References

1. Costa RA, Skaf M, Melo LA Jr, et al. Retinal assessment using optical coherence tomography. *Prog Retin Eye Res*. 2006;25:325–353.
2. Drexler W, Fujimoto JG. State-of-the-art retinal optical coherence tomography. *Prog Retin Eye Res*. 2008;27:45–88.
3. Wojtkowski M, Kaluzny B, Zawadzki RJ. New directions in ophthalmic optical coherence tomography. *Optom Vis Sci*. 2012;89:524–542.
4. von Ruckmann A, Fitzke FW, Bird AC. Distribution of fundus autofluorescence with a scanning laser ophthalmoscope. *Br J Ophthalmol*. 1995;79:407–412.
5. Tsunoda K, Oguchi Y, Hanazono G, Tanifuji M. Mapping cone- and rod-induced retinal responsiveness in macaque retina by optical imaging. *Invest Ophthalmol Vis Sci*. 2004;45:3820–3826.
6. Hanazono G, Tsunoda K, Shinoda K, Tsubota K, Miyake Y, Tanifuji M. Intrinsic signal imaging in macaque retina reveals different types of flash-induced light reflectance changes of different origins. *Invest Ophthalmol Vis Sci*. 2007;48:2903–2912.
7. Hanazono G, Tsunoda K, Kazato Y, Tsubota K, Tanifuji M. Evaluating neural activity of retinal ganglion cells by flash-evoked intrinsic signal imaging in macaque retina. *Invest Ophthalmol Vis Sci*. 2008;49:4655–4663.
8. Inomata K, Tsunoda K, Hanazono G, et al. Distribution of retinal responses evoked by transscleral electrical stimulation detected by intrinsic signal imaging in macaque monkeys. *Invest Ophthalmol Vis Sci*. 2008;49:2193–2200.
9. Tsunoda K, Hanazono G, Inomata K, Kazato Y, Suzuki W, Tanifuji M. Origins of retinal intrinsic signals: a series of experiments on retinas of macaque monkeys. *Jpn J Ophthalmol*. 2009;53:297–314.
10. Crittin M, Riva CE. Functional imaging of the human papilla and peripapillary region based on flicker-induced reflectance changes. *Neurosci Lett*. 2004;360:141–144.
11. Abramoff MD, Kwon YH, Ts'o D, et al. Visual stimulus-induced changes in human near-infrared fundus reflectance. *Invest Ophthalmol Vis Sci*. 2006;47:715–721.
12. Grieve K, Roorda A. Intrinsic signals from human cone photoreceptors. *Invest Ophthalmol Vis Sci*. 2008;49:713–719.
13. Yao XC, Zhao YB. Optical dissection of stimulus-evoked retinal activation. *Opt Express*. 2008;16:12446–12459.
14. Lucas BC, Driller J, Iwamoto T, Silverman RH, Lizzi FL, Coleman DJ. Ultrasonically induced disruption and hemolysis of vitreous hemorrhages. *Ultrasound Med Biol*. 1989;15:29–37.
15. Li YC, Strang C, Amthor FR, et al. Parallel optical monitoring of visual signal propagation from the photoreceptors to the inner retina layers. *Opt Lett*. 2010;35:1810–1812.
16. Zhang QX, Lu RW, Curcio CA, Yao XC. In vivo confocal intrinsic optical signal identification of localized retinal dysfunction. *Invest Ophthalmol Vis Sci*. 2012;53:8139–8145.
17. Nelson DA, Krupsky S, Pollack A, et al. Special report: noninvasive multi-parameter functional optical imaging of the eye. *Ophthalmic Surg Lasers Imaging*. 2005;36:57–66.
18. Okawa Y, Fujikado T, Miyoshi T, et al. Optical imaging to evaluate retinal activation by electrical currents using suprachoroidal-transretinal stimulation. *Invest Ophthalmol Vis Sci*. 2007;48:4777–4784.
19. Maheswari RU, Takaoka H, Homma R, Kadono H, Tanifuji M. Implementation of optical coherence tomography (OCT) in visualization of functional structures of cat visual cortex. *Opt Commun*. 2002;202:47–54.

20. Maheswari RU, Takaoka H, Kadono H, Homma R, Tanifuji M. Novel functional imaging technique from brain surface with optical coherence tomography enabling visualization of depth resolved functional structure in vivo. *J Neurosci Methods*. 2003;124:83–92.
21. Aguirre AD, Chen Y, Fujimoto JG, Ruvinskaya L, Devor A, Boas DA. Depth-resolved imaging of functional activation in the rat cerebral cortex using optical coherence tomography. *Opt Lett*. 2006;31:3459–3461.
22. Yao XC, Yamauchi A, Perry B, George JS. Rapid optical coherence tomography and recording functional scattering changes from activated frog retina. *Appl Opt*. 2005;44:2019–2023.
23. Bizheva K, Pflug R, Hermann B, et al. Optophysiology: depth-resolved probing of retinal physiology with functional ultrahigh-resolution optical coherence tomography. *Proc Natl Acad Sci U S A*. 2006;103:5066–5071.
24. Srinivasan VJ, Wojtkowski M, Fujimoto JG, Duker JS. In vivo measurement of retinal physiology with high-speed ultrahigh-resolution optical coherence tomography. *Opt Lett*. 2006;31:2308–2310.
25. Tumlinson A, Hermann B, Hofer B, et al. Techniques for extraction of depth-resolved in vivo human retinal intrinsic optical signals with optical coherence tomography. *Jpn J Ophthalmol*. 2009;53:315–326.
26. Srinivasan VJ, Chen Y, Duker JS, Fujimoto JG. In vivo functional imaging of intrinsic scattering changes in the human retina with high-speed ultrahigh resolution OCT. *Opt Express*. 2009;17:3861–3877.
27. Rha J, Schroeder B, Godara P, Carroll J. Variable optical activation of human cone photoreceptors visualized using a short coherence light source. *Opt Lett*. 2009;34:3782–3784.
28. Schmoll T, Kolbitsch C, Leitgeb RA. In vivo functional retinal optical coherence tomography. *J Biomed Opt*. 2010;15:041513.
29. Moayed AA, Hariri S, Choh V, Bizheva K. In vivo imaging of intrinsic optical signals in chicken retina with functional optical coherence tomography. *Opt Lett*. 2011;36:4575–4577.
30. Moayed A, Hariri S, Choh V, Bizheva K. Correlation of visually evoked intrinsic optical signals and electroretinograms recorded from chicken retina with a combined functional optical coherence tomography and electroretinography system. *J Biomed Opt*. 2012;17:016011.
31. Brown PK, Wald G. Visual pigments in human and monkey retinas. *Nature*. 1963;200:37–43.
32. Bowmaker JK, Dartnall HJ, Mollon JD. Microspectrophotometric demonstration of four classes of photoreceptor in an old world primate, Macaca fascicularis. *J Physiol*. 1980;298:131–143.
33. White B, Pierce M, Nassif N, et al. In vivo dynamic human retinal blood flow imaging using ultra-high-speed spectral domain optical coherence tomography. *Opt Express*. 2003;11:3490–3497.
34. Jonnal RS, Besecker JR, Derby JC, et al. Imaging outer segment renewal in living human cone photoreceptors. *Opt Express*. 2010;18:5257–5270.
35. Fernandez EJ, Hermann B, Povazay B, et al. Ultrahigh resolution optical coherence tomography and pancorrection for cellular imaging of the living human retina. *Opt Express*. 2008;16:11083–11094.
36. Spaide RF, Curcio CA. Anatomical correlates to the bands seen in the outer retina by optical coherence tomography: literature review and model. *Retina*. 2011;31:1609–1619.
37. Hanazono G, Tsunoda K, Kazato Y, Suzuki W, Tanifuji M. Functional topography of rod and cone photoreceptors in macaque retina determined by retinal densitometry. *Invest Ophthalmol Vis Sci*. 2012;53:2796–2803.
38. Packer O, Hendrickson AE, Curcio CA. Photoreceptor topography of the retina in the adult pigtail macaque (Macaca nemestrina). *J Comp Neurol*. 1989;288:165–183.
39. Curcio CA, Sloan KR, Kalina RE, Hendrickson AE. Human photoreceptor topography. *J Comp Neurol*. 1990;292:497–523.
40. Snodderly DM, Weinhaus RS, Choi JC. Neural vascular relationships in central retina of macaque monkeys (Macaca-fascicularis). *J Neurosci*. 1992;12:1169–1193.
41. Makita S, Fabritius T, Yasuno Y. Quantitative retinal-blood flow measurement with three-dimensional vessel geometry determination using ultrahigh-resolution Doppler optical coherence angiography. *Opt Lett*. 2008;33:836–838.
42. Wang Y, Lu A, Gil-Flamer J, Tan O, Izatt JA, Huang D. Measurement of total blood flow in the normal human retina using Doppler Fourier-domain optical coherence tomography. *Br J Ophthalmol*. 2009;93:634–637.
43. Stepnoski RA, Laporta A, Raccuiabehling F, Blonder GE, Slusher RE, Kleinfeld D. Noninvasive detection of changes in membrane-potential in cultured neurons by light-scattering. *Proc Natl Acad Sci U S A*. 1991;88:9382–9386.
44. Dawis SM, Rossetto M. Light-evoked changes in near-infrared transmission by the ON and OFF channels of the anuran retina. *Vis Neurosci*. 1993;10:687–692.
45. Zonta M, Angulo MC, Gobbo S, et al. Neuron-to-astrocyte signaling is central to the dynamic control of brain microcirculation. *Nature Neurosci*. 2003;6:43–50.
46. Mulligan SJ, MacVicar BA. Calcium transients in astrocyte endfeet cause cerebrovascular constrictions. *Nature*. 2004;431:195–199.
47. Kotliar KE, Vilser W, Nagel E, Lanzl IM. Retinal vessel reaction in response to chromatic flickering light. *Graefes Arch Clin Exp Ophthalmol*. 2004;242:377–392.
48. Newman EA. Calcium increases in retinal glial cells evoked by light-induced neuronal activity. *J Neurosci*. 2005;25:5502–5510.
49. Metea MR, Newman EA. Glial cells dilate and constrict blood vessels: a mechanism of neurovascular coupling. *J Neurosci*. 2006;26:2862–2870.
50. Riva CE, Harino S, Shonat RD, Petrig BL. Flicker evoked increase in optic nerve head blood flow in anesthetized cats. *Neurosci Lett*. 1991;128:291–296.
51. Lujan BJ, Roorda A, Knighton RW, Carroll J. Revealing Henle's fiber layer using spectral domain optical coherence tomography. *Invest Ophthalmol Vis Sci*. 2011;52:1486–1492.
52. Weinhaus RS, Burke JM, Delori FC, Snodderly DM. Comparison of fluorescein angiography with microvascular anatomy of macaque retinas. *Exp Eye Res*. 1995;61:1–16.

Investigative Ophthalmology & Visual Science